^{1}H and ^{13}C NMR Assignment of Sunitinib Malate in Aqueous Media

Myungjo J. Kim, Jong Hoa Ok, Chul Hwan Kim, and Joo Young Oh

R&D Center, SCAI Therapeutics, Inc., Daejeon 34013, Republic of Korea

mjk@scaitrx.com

[Abstract]

Despite expanding therapeutic application of sunitinib and advances in its formulation, pharmacochemical and spectroscopical study on its aqueous solution is rather insufficient due to poor solubility of its base or salt form. In this report, ^{1}H (900 MHz) and ^{13}C (225 MHz) NMR spectra of sunitinib malate in H_2O/D_2O=9/1 have been analyzed, whose spectral peaks have been assigned to each hydrogen and carbon atom, assisted by a combination of two-dimensional homo- and heteronuclear NMR: COSY, HSQC-DEPT, and HMBC. The assignment of labile H-N hydrogens in ^{1}H NMR spectrum is of particular interest in aqueous media, where such labile hydrogens could be potentially affected by intermolecular interactions (*e.g.*, hydrogen bonding) with co-solvated constituents. Peak splitting patterns and corresponding $^{n}J_{H-H}$, $^{n}J_{H-F}$, and $^{n}J_{C-F}$ coupling constants observed in each assigned spectrum have been jointly discussed, and $^{n}J_{C-F}$ coupling constants were compared to those taken in DMSO-d6.

Sunitinib is a versatile tyrosine kinase inhibitor, sold under the brand name Sutent® by Pfizer as its malate salt form.[1] It is currently used to treat renal cell carcinoma and gastrointestinal stromal tumors through its antitumor and antiangiogenic activities, while more of its activities and applications are being explored. Further research endeavors regarding its broader range of application against leukemia and solid tumors (*e.g.*, non-small-cell lung cancer, pancreatic neuroendocrine tumors, and metastatic breast cancer) are currently ongoing.[2] Besides oncological utilization, treatment of age-related macular degeneration is one of its other notable applications which led us to constitute aqueously dispersed sunitinib malate in an eyedrop formulation recently.[3] As of January 2022, 27 clinical trials in 40 countries for sunitinib alone or in combination with other drug(s), are under way for novel applications towards paraganglioma, thymoma, prostate cancer, stomach neoplasm, and more;[4] allowing the medicinal research community to expect greater therapeutic potential.

Given the expanding application of sunitinib base or its malate salt form, adequate pharmaceutical formulation research as well as pharmacochemical study should follow accordingly. For instance, though there have been various attempts to constitute sunitinib malate into novel pharmaceutical formulations, solubility issue that the ionic compound being poorly soluble in water[5] has been a major bottleneck. Recent reports describe different types of nanoparticle,[6] suspension,[7] and micelle[8] formulations, where spectroscopical method such as NMR is particularly important to determine intermolecular interaction between pharmaceutical ingredients. However, on its ^{1}H and ^{13}C NMR spectra, each spectral peak signal has not been clearly assigned to each hydrogen and carbon atom in its chemical structure. There have only been a few reports of incomplete assignments in $CDCl_3$ and DMSO-d6 to date.[9,10] The assignment of labile H–N hydrogens is of particular interest in aqueous formulations, in order to identify which H–N bond is responsible for intermolecular interaction (*e.g.*, hydrogen bonding) with solvated salt, additive, and solvent. Herein, we report the ^{1}H and ^{13}C NMR assignment of sunitinib malate in aqueous media, including the assignment of major labile H–N hydrogens.

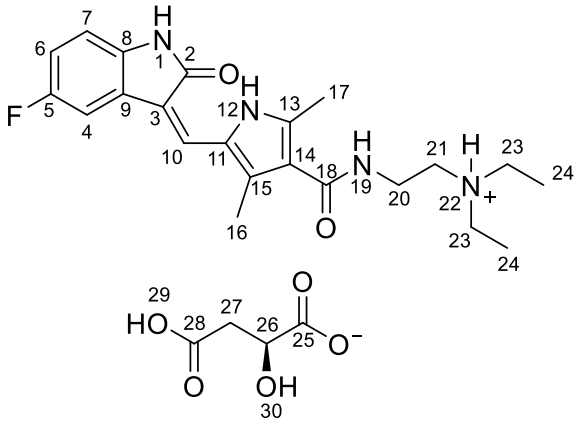

Figure 1. Labelling of nitrogen and oxygen atoms with labile hydrogens, and skeletal carbon atoms of sunitinib malate.

As shown in **Figure 1**, nitrogen and oxygen atoms attached to labile hydrogens — H–N_1, H–N_{12}, H–N_{19}, H–N_{22}, H–O_{29}, and H–O_{30} — as well as skeletal carbon atoms were labelled. In order to acquire ^{1}H spectrum in aqueous media with no loss of labile hydrogen peaks, H_2O solvent with additional D_2O (10%, v/v) was used instead of pure D_2O, where water-suppression method was used. As a result, spectral peaks of labile H-N hydrogens H-N_1, H–N_{12}, and H–N_{19} were well observed with the peak integration of 0.43H, 0.85H, and 0.88H, respectively (**Figure S1**). On the other hand, H–O_{29}, H–O_{30}, and H–N_{22} were not observed where the first two underwent rapid deuterium-hydrogen

exchange.

It is notable that none of the aromatic peaks were overlapped by each other in contrast to the previously reported spectrum acquired in DMSO-d6.[9] Chemical shift of the C_{16} and C_{17} methyl groups on the pyrrole ring (at around 1.88 ppm and 1.86 ppm) were much lower than those from the spectrum acquired in DMSO-d6 so that they did not overlap with two H–C_{27} doublets of malate at around 2.72 and 2.54 ppm as well. Due to the baseline affected by the water-suppression near 4.80 ppm, peak integration for H–C_{26} was rather inaccurate (0.73H). H–C_{23} quartet at 3.22 ppm and H–C_{21} triplet at 3.21 ppm with similar intensities, were found to partially overlap each other to appear as a quintet-like structure as shown in **Figure 2(a)**. Aromatic hydrogen peaks of the indolinone ring, H–C_4, H–C_6, and H–C_7, as well as *exo*-cyclic vinyl H–C_{10}, are shown in **Figure 2(b)**, where the first three were split into doublet-of-doublets and a triplet-of-doublet, due to a combination of hydrogen-fluorine and hydrogen-hydrogen couplings across the ring. The J-coupling constants were estimated to be $^3J_{H\text{-}F}$ = 8.92 Hz (*ortho*, H–C_4), $^4J_{H\text{-}H}$ = 2.43 Hz (*meta*, H–C_4), $^3J_{H\text{-}F}$ = 8.67 Hz (*ortho*, H–C_6), $^4J_{H\text{-}H}$ = 2.17 Hz (*meta*, H–C_6), $^3J_{H\text{-}H}$ = 8.23 Hz (*ortho*, H–C_6), $^4J_{H\text{-}F}$ = 4.24 Hz (*meta*, H–C_7), and $^3J_{H\text{-}H}$ = 7.90 Hz (*ortho*, H–C_7).

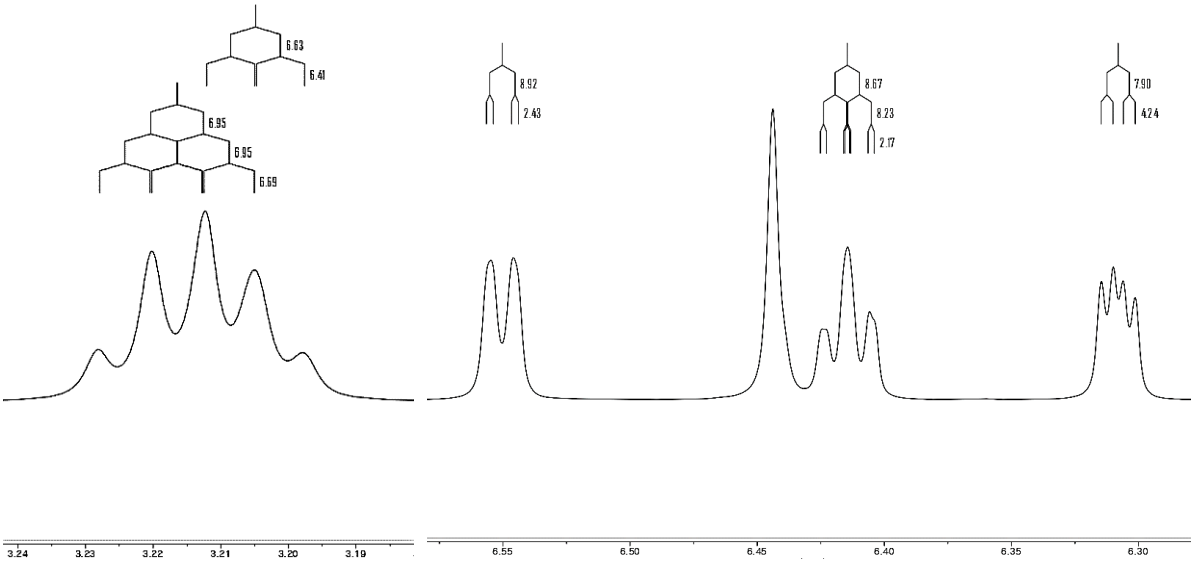

Figure 2. (a) J-coupling tree diagrams of partially overlapped H–C_{23} (quartet) and H–C_{21} (triplet) peaks (left). (b) J-coupling tree diagrams of H–C_4 (doublet-of-doublet), H–C_6 (triplet-of-doublet), and H–C_7 (doublet-of-doublet) peaks in that order from the downfield (right). (Chemical shift: ppm)

^{13}C carbon NMR was acquired in the same environment which gave good signal-to-noise ratios with respect to peaks for carbonyl carbons and aromatic carbons that do not possess any hydrogen

atom (**Figure S2**). Carbon-fluorine coupling constants from the aromatic hydrogen peaks of the indolinone ring, were estimated to be $^{1}J_{C\text{-}F}$ = 235.62 Hz (*ipso*, C_5), $^{2}J_{C\text{-}F}$ = 24.78 Hz (*ortho*, C_4), $^{2}J_{C\text{-}F}$ = 24.19 Hz (*ortho*, C_6), $^{3}J_{C\text{-}F}$ = 8.57 Hz (*meta*, C_7), and $^{3}J_{C\text{-}F}$ = 9.01 Hz (*meta*, C_9), where no *para* coupling was observed (**Figure 3**). It is uncertain that singlets of *ipso* carbon doublet have particularly asymmetric peak intensities throughout repeated experiments, where that of ^{13}C spectrum acquired in DMSO-d6 showed similar singlet peak intensities within the corresponding doublet. In-house measurement of the coupling constants in DMSO-d6 at 100 MHz resulted in $^{1}J_{C\text{-}F}$ = 234.33 Hz (*ipso*, C_5), $^{2}J_{C\text{-}F}$ = 25.52 Hz (*ortho*, C_4), $^{2}J_{C\text{-}F}$ = 24.21 Hz (*ortho*, C_6), $^{3}J_{C\text{-}F}$ = 8.52 Hz (*meta*, C_7), $^{3}J_{C\text{-}F}$ = 9.53 Hz (*meta*, C_9), and $^{4}J_{C\text{-}F}$ = 3.09 Hz (*para*, C_8) (**Figure S6**).

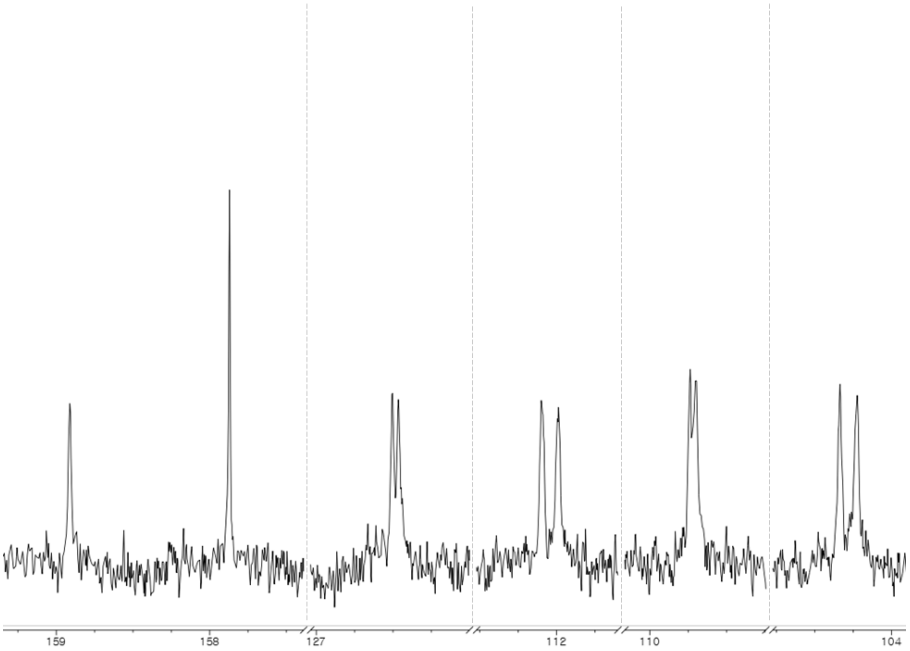

Figure 3. Split ^{13}C peaks of aromatic carbons *ipso*, *ortho*, and *meta* to the fluorine atom: C_5 (*ipso*), C_9(*meta*), C_6(*ortho*), C_7(*meta*), and C_4(*ortho*) in that order from the downfield. (Chemical shift: ppm)

Throughout a HSQC-DEPT experiment, we could easily differentiate methylene carbons (anti-phase signals) between 3.60 and 2.40 ppm from the rest of the spectrum: CH_2 moieties on the ammonium tether (H–C_{20}, H–C_{21}, and H–C_{23}) and the malate backbone (H–C_{27}) (**Figure S3**). Methyl groups at the end of the tether and on the pyrrole ring, showed the in-phase signals in the upfield region (2.00 – 1.10 ppm). Each aromatic hydrogen peak was assigned to the adjacent carbon within the indolinone moiety (H–C_4, H–C_6, and H–C_7) as well as *exo*-cyclic vinyl hydrogen to its skeletal carbon (H–C_{10}), where they exhibited in-phase signals on the two-dimensional spectrum as well. COSY spectrum (**Figure S4**) showed clear off-diagonal signals to confirm the *ortho* relationship between

104 H–C_6 and H–C_7, and to confirm the connectivity through the ammonium tether.

105

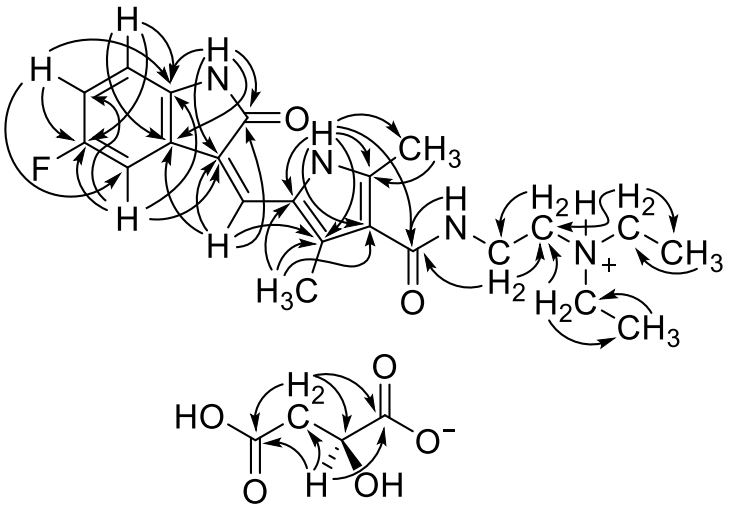

106

107 **Figure 4**. Summary of HMBC correlations within sunitinib malate in aqueous media.

108

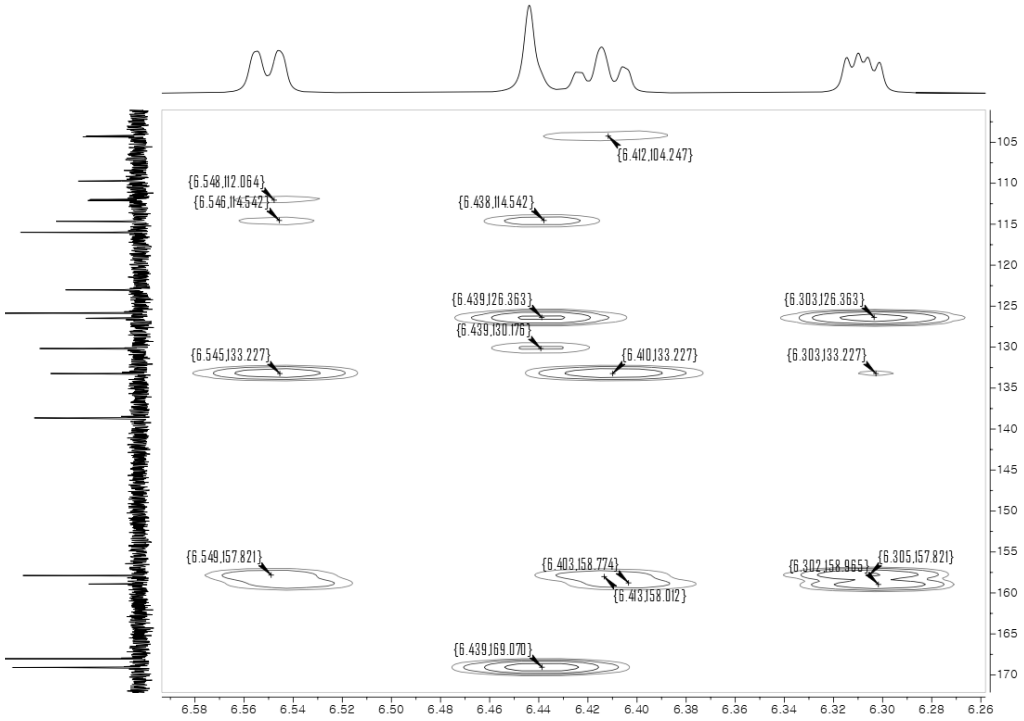

109

110 **Figure 5**. Key HMBC correlations from aromatic hydrogen peaks and *exo*-cyclic vinyl hydrogen peak.

111 (Chemical shift: ppm)

112

Table 1. Summarized NMR peak assignment table of sunitinib malate in H_2O/D_2O=9/1 (v/v).

$^1H/^{13}C$ Assignment	Chemical Shift[a] (δ_H) (ppm)	Chemical Shift[a] (δ_C) (ppm)	J-Coupling Constants[b] (Hz)	HSQC-DEPT Correlations[c]	HMBC Correlations	COSY Correlations
1	9.582				C_2, C_3, C_8, C_9	
2		169.097				
3		114.645				
4	6.550(dd)	104.281(d)	2.43, 8.92, (24.78)	C_4 (+)	C_3, C_5, C_6, C_8	
5		158.392(d)	(235.62)			
6	6.414(td)	112.042(d)	2.17, 8.23, 8.67, (24.19)	C_6 (+)	C_4, C_5, C_8	H-C_7
7	6.308(dd)	109.718(d)	4.24, 7.90, (8.57)	C_7 (+)	C_5, C_8, C_9	H-C_6
8		133.221				
9		126.484(d)	(9.01)			
10	6.444	123.016		C_{10} (+)	C_2, C_3, C_9, C_{15}	
11		125.866				
12	12.293				C_{11}, C_{13}, C_{14}, C_{15}, C_{17}, C_{18}	
13		138.641				
14		115.996				
15		130.169				
16	1.875	10.053		C_{16} (+)	C_{11}, C_{14}, C_{15}	
17	1.860	13.093		C_{17} (+)	C_{13}	
18		168.029				
19	7.042				C_{18}	H-C_{20}
20	3.522(q)	34.782	6.42, 6.50, 6.50	C_{20} (−)	C_{18}, C_{21}	H-C_{19}, H-C_{21}
21	3.205(t)	51.180	6.41, 6.63	C_{21} (−)	C_{20}	H-C_{20}
22						
23	3.216(q)	48.251	6.69, 6.95, 6.95	C_{23} (−)	C_{21}, C_{24}	H-C_{24}
24	1.261(t)	8.454	7.19	C_{24} (+)	C_{23}	H-C_{23}
25[d]		179.153				
26	4.296(dd)	68.676	4.32, 8.10	C_{26} (+)	C_{25}, C_{27}, C_{28}	H-C_{27}
27	2.724(dd); 2.535(dd)	40.248	4.31, 15.97; 8.11, 15.97	C_{27} (−)	C_{25}, C_{26}, C_{28}	H-C_{26}
28[d]		176.502				

[a]Singlet unless otherwise stated; d: doublet; t: triplet; q: quartet; dd: doublet-of-doublet; td: triplet-of-doublet. [b]J-coupling constant in ^{13}C NMR is described in parenthesis. [c]In-phase and anti-phase signals are denoted by (+) and (−) signs, respectively. [d]Differentiation between two carbonyl carbons of malate (C_{25} and C_{28}) was not viable due to the presence of both three-bond correlations ($^3J_{C\text{-}H}$) from H_{26} and H_{27}.

HMBC spectrum (**Figure S5**) confirmed the connectivity throughout the structure via crucial long-range correlations as summarized by arrows in **Figure 4**. HMBC correlations from the aromatic hydrogen peaks of the indolinone ring and *exo*-cyclic vinyl hydrogen peak are shown in **Figure 5** where key multi-bond couplings across the indolinone ring are exhibited. However, ^{13}C peak

assignment of pyrrole ring carbons C_{11}, C_{14}, and C_{15}, is not fully settled unfortunately, due to (1) a missing long-range coupling from H-C_{17} and/or H-N_{19} for the absolute determination of the C_{14} peak, and (2) a challenging differentiation of $^{2}J_{C\text{-}H}$ from long-range couplings as HMBC-RELAY, H2BC, and ^{2}J,^{3}J-HMBC could not be utilized for non-hydrogenated carbons.[11] Since optimization of pulse sequence length was not viable, the HMBC correlation from H_{10} into the pyrrole ring was assumed to be a $^{3}J_{C\text{-}H}$ coupling, as $^{2}J_{C\text{-}H}$ couplings often tend to be weak or missing in conventional HMBC. Summarized peak table for each hydrogen and carbon atom assigned, including peak multiplicity, J-coupling constant, and HSQC-DEPT/HMBC/COSY correlations, is provided in **Table 1**.

In conclusion, we report the first complete ^{1}H and ^{13}C NMR assignment of sunitinib malate in aqueous media, assisted by a combination of two-dimensional homo- and hetero-nuclear NMR, COSY, HSQC-DEPT, and HMBC. H_2O/D_2O co-solvent system was used in order to identify major labile H–N hydrogens which could potentially play crucial roles in aqueous intermolecular interactions. Peak splitting patterns in each assigned spectrum are also discussed as well as the corresponding $^{n}J_{H\text{-}H}$, $^{n}J_{C\text{-}H}$, and $^{n}J_{C\text{-}F}$ coupling constants measured. Each assigned spectrum showed substantial difference from those acquired in aprotic solvents in respect of chemical shift and peak splitting. We believe that the assignment would be useful for further formulation research of sunitinib malate and relevant pharmaceutical moieties.

[Acknowledgement]

This work is supported by SCAI Therapeutics, Inc. We are grateful to Eun-Hee Kim and Hae-Kap Cheong (Korea Basic Science Institute) for the acquisition of the NMR spectra. We thank Kyoung-Hee Kim and Geewoo Nam (SCAI Therapeutics Inc.) for fruitful discussions.

[Associated Content]

Experimental procedure and NMR spectra with detailed acquisition parameters are available in Supporting Information via ChemRxiv website (https://chemrxiv.org).

[References]

[1]Faivre *et al., Nature Reviews Drug Discovery* **2007**, *6*, 734.

[2](a) Fiedler *et al., British Journal of Haematology* **2015**, *169*, 694. (b) Novello *et. al., Journal of Thoracic Oncology* **2011**, *6*, 1260. (c) Faivre *et. al., Annals of Oncology* **2017**, *28*, 339. (d) Elgebaly

et. al., Breast Disease **2016**, *36*, 91.

[3](a) Kim *et al., Investigative Ophthalmology & Visual Science* **2021**, *62*, 447. (b) Kim *et al., American Academy of Ophthalmology 2020 Annual Meeting*, Las Vegas, NV, **2020**, PO441.

[4] https://clinicaltrials.gov. Accessed on January 19th, 2022. [Advanced search details] Status (Recruitment): "Active, not recruiting"; Intervention/treatment: "sunitinib"; irrelevant search results excluded.

[5]Sangwan *et al., International Research Journal of Pure & Applied Chemistry* **2015**, *5*, 352. Note: It is also notable that novel salt forms of sunitinib with adipate and nicotinate show higher solubility in water than that of malate salt form.

[6](a) Joseph *et al., International Journal of Biological Macromolecules* **2016**, *82*, 952. (b) Bhatt *et al., AAPS PharmSciTech* **2019**, *20*, 281.

[7]Navid *et al., The Annals of Pharmacotherapy* **2008**, 42, 962.

[8]Streets *et al., Scientia Pharmaceutica* **2020**, *88*, 30.

[9](a) Kassem *et al.*, Chapter 9. In *Profiles of Drug Substances, Excipients and Related Methodology* Volume 37, Brittain Eds., Elsevier, **2012**, 363. (b) Manley *et al., Journal of Organic Chemistry* **2003**, *68*, 6447. (c) Wang *et al., Bioorganic & Medicinal Chemistry Letter* **2005**, *15*, 4380.

[10] Following article reports comprehensive physicochemical characteristics of sunitinib malate, however the assigned ^{1}H, ^{13}C, and ^{15}N NMR spectra acquired in DMSO-d6 are not provided: Sidoryk *et al., Journal of Pharmaceutical Sciences* **2013**, *102*, 706.

[11](a) Saurí *et al., Concepts in Magnetic Resonance Part A* **2016**, *44A*, 227. (b) Nyberg *et al., Journal of the American Chemical Society* **2005**, *127*, 6154.